

Electronic Supporting Information

Submitted to Polymer Chemistry

A Cyclic Azobenzophane-Based Smart Polymer for Chiroptical Switches

Jinjie Lu,^a Ganquan Jiang,^a Zhengbiao Zhang,^a Wei Zhang,^a Yonggang Yang,^a Yong
Wang,^{*b} Nianchen Zhou,^{*a} Xiulin Zhu^{*a}

^a Jiangsu Key Laboratory of Advanced Functional Polymer Design and Application
College of Chemistry, Chemical Engineering and Materials Science, Soochow
University, Suzhou, 215123, P. R. China. E-mail: xlzhu@suda.edu.cn.;
nczhou@suda.edu.cn.

^b Key Laboratory of Organic Synthesis of Jiangsu Province College of Chemistry,
Chemical Engineering and Materials Science, Soochow University, Suzhou 215123, P.
R. China. E-mail: yowang@suda.edu.cn.

Characterizations

The number-average molecular weight (M_n) and polydispersity ($M_w/M_n = \text{PDI}$) of the polymer was determined using a size exclusion column TOSOH HLC-8320 equipped with refractive-index and UV detectors using two TSKgel Super Mutipore HZ-N (4.6×150 mm, $3 \mu\text{m}$ beads size) columns arranged in series, and it can separate polymers in the molecular weight range $500\text{-}1.9 \times 10^5$ g/mol. Tetrahydrofuran (THF) was used as the eluent at a flow rate of 0.35 mL min^{-1} at 40°C . Data acquisition was performed using EcoSEC software, and molecular weights were calculated with polystyrene (PS) standards.

The CD spectra were recorded simultaneously at 25°C on a JASCO J-815 spectropolarimeter equipped with a Peltier-controlled housing unit using an SQ-grade cuvette, with a path length of 10 mm (with a scanning rate of 100 nm/min , a bandwidth of 2 nm and a response time of 1 s, using a single accumulation).

Optical rotations were measured on an Autopol IV polarimeter (Rudolf Research Analytical, Flanders, USA) at 25°C in chloroform and $[\alpha]_D$ values are given in $10^{-1} \text{ deg cm}^2 \text{ g}^{-1}$.

All ^1H NMR spectra and ^{13}C NMR spectra were collected using a Bruker nuclear magnetic resonance instrument (300 MHz) using tetramethylsilane (TMS) as the internal standard at room temperature. NMR samples were prepared with concentrations of 10-20 mg/mL in CDCl_3 or $\text{DMSO-}d_6$. The ^1H NMR spectra were referenced to δ 7.26 ppm in CDCl_3 or δ 2.50 ppm in $\text{DMSO-}d_6$.

Ultraviolet visible (UV-vis) absorption spectra of the samples were recorded on a Shimadzu UV-2600 spectrophotometer at room temperature.

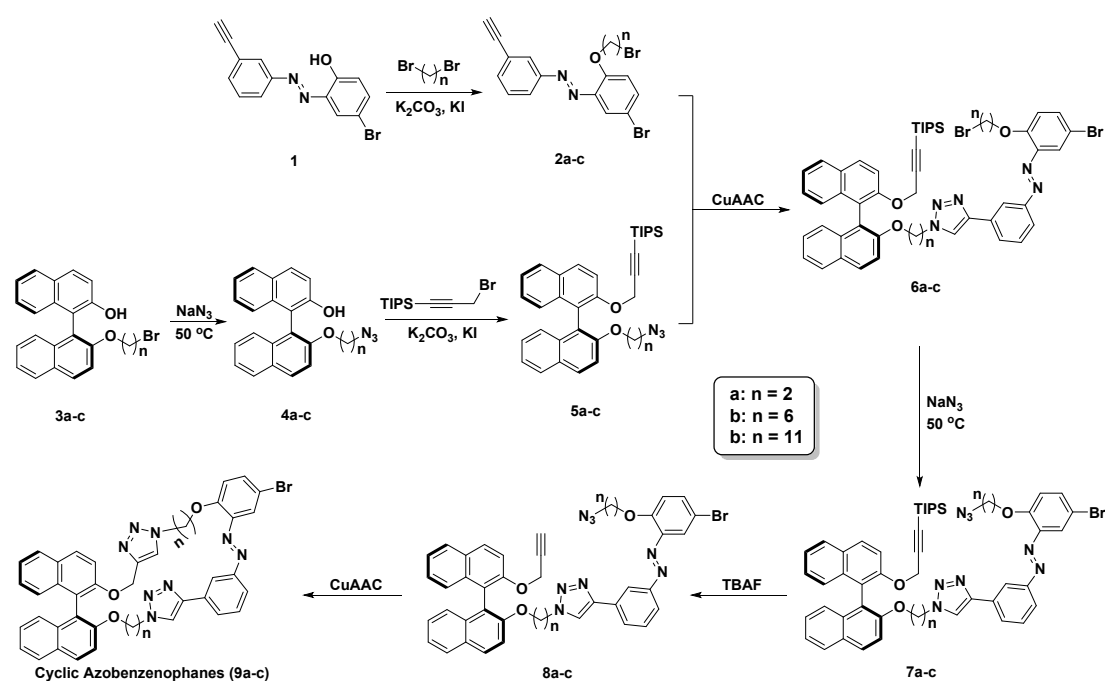
The elemental analysis was performed on a Vario EL elemental analysis instrument (Elementar (Donaustraße, Hanau, Germany)).

High-resolution mass spectra (HRMS) were recorded on a Bruker Esquire LC/Ion Trap Mass Spectrometer and JEOL/HX-110.

Melting points (T_m) were recorded on an Electrothermal digital melting point apparatus (SGW X4) and were uncorrected.

Materials

(S)-1,1'-Bi-2-naphthol (S-BINOL, 98%, Suzhou Soochiral chemistry, China), 4-vinylphenylboronic acid (VPB, 98%, Suzhou Soochiral chemistry), tetrakis (triphenylphosphine)-palladium(0) (97.0%, Sigma-Aldrich), p-bromophenol (97.0%, J&K), 3-ethynylaniline (>98%, Aldrich), 2-bromoethanol (98%, Energy Chemical), 6-bromohexanol (97%, Energy Chemical), 11-bromoundecanol (97%, Energy Chemical), diethyl azodicarboxylate (DEAD, 98%, Energy Chemical), tetrabutylammonium fluoride (TBAF) solution (1M in THF, Energy Chemical), sodium azide (>99.5%, Aldrich), (3-bromoprop-1-yn-1-yl) triisopropylsilane (Bengbu Nako Chemical Co., Ltd., China). Azobisisobutyronitrile (AIBN, 99%, Energy Chemical) was recrystallized three times from ethanol and dried in vacuum at room temperature overnight. *N,N,N',N'',N''*-Pentamethyldiethylenetriamine (PMDETA, 98%, J&K) was distilled under reduced pressure before used. Other reagents mentioned in this article were used directly after purchased without further purification. And all solvents were used as received.



Scheme S1. Synthetic routes of three cyclic azobenzenophanes (9a, 9b and 9c) with different methylene spacers ($n = 2, 6, 11$). The axial chirality of binaphthyl is *S*.

Synthesis of 4-Bromo-2-((3-ethynylphenyl)diazenyl)phenol (1)

This compound was synthesized according to literature procedure.¹

Synthesis of 1-(5-bromo-2-(2-bromoethoxy)phenyl)-2-(3-ethynylphenyl)diazene (2a)

A 250 mL round bottomed flask was charged with 1 (3.00 g, 10.0 mmol), triphenylphosphine (3.93 g, 15.0 mmol) and THF of 40 mL, then a mixture of 2-bromoethanol (1.10 mL, 15.0 mmol) and DEAD (7.16 g, 15.0 mmol) was added dropwise to the mixture. The reaction mixture was slowly warmed to reflux. After 15 h, the mixture was cooled to ambient temperature and the solvent was removed by rotary evaporation. The crude product was chromatographed on a silica gel column (petroleum ether/ethyl acetate) to afford 2a as red solid in 75% yield. ¹H NMR (300 MHz, CDCl₃), δ(TMS, ppm): 8.04 (s, 1H, ArH), 7.92 (d, 1H, ArH), 7.83 (d, 1H, ArH), 7.62 (d, 1H, ArH), 7.55-7.45 (m, 2H, ArH), 7.04 (d, 1H, ArH), 4.53 (t, 2H, ArOCH₂-), 3.74 (t, 2H, BrCH₂-), 3.15 (s, 1H, -C≡CH).

Synthesis of 1-(5-bromo-2-((6-bromohexyl)oxy)phenyl)-2-(3-ethynylphenyl)diazene (2b)

2b was synthesized in a similar manner to that for 2a with the exception that 6-bromohexanol was used. 83% yield, red solid. ¹H NMR (300 MHz, CDCl₃), δ(TMS, ppm): 8.01 (s, 1H, ArH), 7.91 (d, 1H, ArH), 7.79 (d, 1H, ArH), 7.60 (d, 1H, ArH), 7.52-7.44 (m, 2H, ArH), 6.98 (d, 1H, ArH), 4.19 (t, 2H, ArOCH₂-), 3.42 (t, 2H, BrCH₂-), 3.15 (s, 1H, -C≡CH), 1.97-1.82 (m, 4H, -OCH₂CH₂, BrCH₂CH₂-), 1.63-1.47 (m, 4H).

Synthesis of 1-(5-bromo-2-((11-bromoundecyl)oxy)phenyl)-2-(3-ethynylphenyl)diazene (2c)

2c was synthesized in a similar manner to that for 2a with the exception that 11-Bromoundecanol was used. 78% yield, red solid. ¹H NMR (300 MHz, CDCl₃), δ(TMS, ppm): 8.05 (d, 1H, ArH), 7.90 (d, 1H, ArH), 7.80 (d, 1H, ArH), 7.60 (d, 1H,

ArH), 7.60-7.43 (m, 3H, ArH), 6.99 (d, 1H, ArH), 4.25-4.05 (m, 4H, ArOCH₂-, BrCH₂-), 3.13 (s, 1H, -C≡CH), 2.00-1.11 (m, 18H).

Synthesis of (*S*)-2'-(2-bromoethoxy)-[1,1'-binaphthalen]-2-ol (3a)

A 250 mL round bottomed flask was charged with S-BINOL (3.00 g, 10.5 mmol), triphenylphosphine (3.30 g, 12.6 mmol) and THF of 40 mL, then a mixture of 2-bromoethanol (0.93 mL, 12.6 mmol) and DEAD (6.01 g, 12.6 mmol) was added dropwise to the mixture. The reaction mixture was slowly warmed to reflux. After several hours, the mixture was cooled to ambient temperature and the solvent was removed by rotary evaporation. The crude product was chromatographed on a silica gel column (petroleum ether /EtOAc) to afford 3a as colorless solid in 52%. ¹H NMR (300 MHz, CDCl₃), δ(TMS, ppm): 8.05-7.92 (m, 4H, naphthyl), 7.50-7.27 (m, 7H, naphthyl), 7.16 (d, 1H, naphthyl), 5.09 (s, 1H, -OH), 4.31-4.16 (m, 2H, -OCH₂-), 3.30 (t, 2H, BrCH₂-).

Synthesis of (*S*)-2'-((6-bromohexyl)oxy)-[1,1'-binaphthalen]-2-ol (3b)

3b was synthesized in a similar manner to that for 3a with the exception that 6-bromohexanol was used. 57% yield, viscous liquid. ¹H NMR (300 MHz, DMSO-*d*₆), δ(TMS, ppm): 9.26 (s, 1H, -OH), 8.11-7.65 (m, 4H, naphthyl), 7.60-7.40 (d, 1H, naphthyl), 7.37-7.07 (m, 5H, naphthyl), 7.03 (d, 1H, naphthyl), 6.88 (d, 1H, naphthyl), 4.08-3.70 (m, 2H, -OCH₂-), 3.35 (t, 2H, BrCH₂-), 4.58-0.65 (m, 8H).

Synthesis of (*S*)-2'-((11-bromoundecyl)oxy)-[1,1'-binaphthalen]-2-ol (3c)

3c was synthesized in a similar manner to that for 3a with the exception that 11-Bromoundecanol was used. 55% yield, viscous liquid. ¹H NMR (300 MHz, CDCl₃), δ(TMS, ppm): 8.03 (d, 1H, naphthyl), 7.95-7.77 (m, 3H, naphthyl), 7.46 (d, 1H, naphthyl), 7.39-7.17 (m, 6H, naphthyl), 7.07 (d, 1H, naphthyl), 4.93 (s, 1H, -OH), 4.05-3.87 (m, 2H, -OCH₂-), 3.43 (t, 2H, BrCH₂-), 1.93-1.77 (m, 2H), 1.50-0.85 (m, 16H).

Synthesis of (S)-(3-((2'-(2-azidoethoxy)-[1,1'-binaphthalen]-2-yl)oxy)prop-1-yn-1-yl)triisopropylsilane (5a)

A 100 mL round bottom flask was charged with a mixed solution of 3a (3.92 g, 10.00 mmol), NaN₃ (1.95 g, 30.0 mmol), and 50mL DMF under magnetic stirring. The reaction mixture was stirred in 50 °C oil-bath for 24 h and then cooled to room temperature. Then deionized water was added to quench the reaction and the mixture was extracted by ethyl acetate. The organic layer was evaporated in a reduced pressure to yield compound 4a as pale yellow viscous liquid in 97.6% yield.

Subsequently, 4a (1.80 g, 5.00 mmol), K₂CO₃ (1.38 g, 10.00 mmol), (3-Bromoprop-1-yn-1-yl) triisopropylsilane (2.74 g, 10 mmol) and 18-crown-6 (50 mg) were mixed in acetone (25 mL). The mixture was refluxed for 20 h and then poured into deionized water (100 mL). The water solution was extracted with ethyl acetate (3 × 100 mL). The organic layer obtained was dried with anhydrous MgSO₄ overnight, filtered, and evaporated in a reduced pressure. The final crude product was purified by column chromatography (silica gel, EtOAc/petroleum ether) to obtain the compound 5a as pale yellow viscous liquid in 83% yield. ¹H NMR (300 MHz, CDCl₃), δ(TMS, ppm): 7.99 (d, 2H, naphthyl), 7.90 (d, 2H, naphthyl), 7.69 (d, 1H, naphthyl), 7.45 (d, 1H, naphthyl), 7.39 (q, 2H, naphthyl), 7.25-7.12 (m, 4H, naphthyl), 4.72 (q, 2H, -CH₂-C≡C-TIPS), 4.15-4.02 (m, 2H, -OCH₂-), 3.20 (t, 2H, N₃CH₂-), 1.02 (s, 21H, ((CH₃)₂CH)₃-Si).

Synthesis of (S)-(3-((2'-((6-azidohexyl)oxy)-[1,1'-binaphthalen]-2-yl)oxy)prop-1-yn-1-yl)triisopropylsilane (5b)

5b was synthesized in a similar manner to that for 5a with 87% yield, viscous liquid. ¹H NMR (300 MHz, CDCl₃), δ(TMS, ppm): 8.02 (d, 1H, naphthyl), 7.93 (d, 1H, naphthyl), 7.85 (d, 2H, naphthyl), 7.55 (d, 1H, naphthyl), 7.33 (q, 2H, naphthyl), 7.22-7.14 (m, 3H, naphthyl), 7.05 (d, 1H, naphthyl), 6.90 (d, 1H, naphthyl), 4.63 (q, 2H, -CH₂-C≡C-TIPS), 4.08-3.86 (m, -OCH₂-), 3.10 (t, 2H, N₃CH₂-), 1.45-1.27 (m, 2H), 1.27-1.10 (m, 2H), 1.08-0.92 (m, 23H), 0.92-0.75 (m, 2H).

Synthesis of (S)-3-((2'-((11-azidoundecyl)oxy)-[1,1'-binaphthalen]-2-yl)oxy)prop-1-yn-1-yl)triisopropylsilane (5c)

5c was synthesized in a similar manner to that for 5a with 78% yield, viscous liquid. ¹H NMR (300 MHz, CDCl₃), δ(TMS, ppm): 7.94 (d, 1H, naphthyl), 7.91 (d, 1H, naphthyl), 7.86 (d, 2H, naphthyl), 7.64 (d, 1H, naphthyl), 7.42 (d, 1H, naphthyl), 7.33-7.27 (m, 2H, naphthyl), 7.21-7.10 (m, 4H, naphthyl), 4.67 (q, 2H, -CH₂-C≡C-TIPS), 4.07-3.84 (m, 2H, -OCH₂-), 3.28 (t, 2H, N₃CH₂-), 1.64 (m, 2H), 1.43-0.79 (m, 37H).

Synthesis of (S)-4-(3-((5-bromo-2-(2-bromoethoxy)phenyl)diazenyl)phenyl)-1-(2-((2'-((3-(triisopropylsilyl)prop-2-yn-1-yl)oxy)-[1,1'-binaphthalen]-2-yl)oxy)ethyl)-1H-1,2,3-triazole (6a)

To a stirred solution of 2a (4.06g, 10 mmol) and PMDETA (21 μL, 0.1 mmol) in CH₂Cl₂ (50 mL), 5a (5.49 g, 10 mmol) was added. This solution was purged with argon for 30 min to remove oxygen, after which Cu(I)Br (14.5 mg, 0.1 mmol) was added and the flask sealed and reacted at 25 °C for 1 h. The solution was then poured into deionized water (100 mL). The organic layer obtained was dried with anhydrous MgSO₄ overnight, filtered, and evaporated in a reduced pressure. The final crude product was purified by column chromatography (silica gel, EtOAc/petroleum ether) to obtain the compound 6a as yellow viscous liquid in 91% yield. ¹H NMR (300 MHz, CDCl₃), δ (TMS, ppm): 8.07 (s, 1H), 8.00-7.87 (m, 5H), 7.76 (d, 1H), 7.70 (d, 1H), 7.62 (q, 3H), 7.39 (t, 2H), 7.25-7.07 (m, 6H), 6.75 (s, 1H), 4.60-4.44 (m, 8H), 3.75 (t, 2H), 0.95 (s, 21H).

Synthesis of (S)-4-(3-((5-bromo-2-((6-bromohexyl)oxy)phenyl)diazenyl)phenyl)-1-(6-((2'-((3-(triisopropylsilyl)prop-2-yn-1-yl)oxy)-[1,1'-binaphthalen]-2-yl)oxy)hexyl)-1H-1,2,3-triazole (6b)

6b was synthesized in a similar manner to that for 6a with the exception that 2b and 5b were used with 88% yield, viscous liquid. ¹H NMR (300 MHz, CDCl₃), δ (TMS, ppm): 8.32 (s, 1H), 8.02 (d, 1H), 7.94 (q, 2H), 7.87-7.81 (m, 4H), 7.64-7.56 (m, 3H),

7.52 (d, 1H), 7.41 (d, 1H), 7.33 (q, 2H), 7.22-7.12 (m, 4H), 6.99 (d, 1H), 4.65 (q, 2H), 4.19 (t, 2H), 4.10 (t, 2H), 4.04-3.87 (m, 2H), 3.39 (t, 2H), 1.99-0.75 (m, 37H).

Synthesis of (S)-4-(3-((5-bromo-2-((11-bromoundecyl)oxy)phenyl)diazenyl)phenyl)-1-(11-((2'-((3-(triisopropylsilyl)prop-2-yn-1-yl)oxy)-[1,1'-binaphthalen]-2-yl)oxy)undecyl)-1H-1,2,3-triazole (6c)

5b was synthesized in a similar manner to that for 5a with the exception that 2c and 5c were used with 88% yield, viscous liquid. ¹H NMR (300 MHz, CDCl₃), δ (TMS, ppm): 8.30 (s, 1H), 8.08 (d, 1H), 7.94-7.80 (m, 7H), 7.63-7.49 (m, 3H), 7.41 (d, 1H), 7.32-7.27 (t, 2H), 7.21-7.09 (m, 4H), 7.00 (d, 1H), 4.66 (q, 2H), 4.44 (t, 2H), 4.19 (t, 2H), 4.00-3.83 (m, 2H), 3.40 (t, 2H), 1.98-0.86 (m, 57H).

Synthesis of (S)-4-(3-((2-(2-azidoethoxy)-5-bromophenyl)diazenyl)phenyl)-1-(2-((2'-(prop-2-yn-1-yloxy)-[1,1'-binaphthalen]-2-yl)oxy)ethyl)-1H-1,2,3-triazole (8a)

A 100 mL round bottom flask was charged with a mixed solution of 6a (4.72 g, 5.00 mmol), NaN₃ (1.00 g, 15.0 mmol), and 20mL DMF under magnetic stirring. The reaction mixture was stirred in 50 °C oil-bath for 24 h and then cooled to room temperature. Then deionized water was added to quench the reaction and the mixture was extracted by ethyl acetate. The organic layer was evaporated in a reduced pressure to yield compound 7a as pale yellow viscous liquid in 92.3% yield.

Subsequently, 7a (4.60 g, 5 mmol) was dissolved in 40 mL of THF and degassed for 30 min. Then, 10 equiv of TBAF (1 M solution in THF) relative to alkyne functions were added at 0 °C and stirred at this temperature for 2 h. Then, the solvent was removed via rotary evaporation and the crude product was purified by column chromatography (silica gel, EtOAc/petroleum ether) to obtain the compound 8a as yellow solid in 80.7% yield. ¹H NMR (300 MHz, CDCl₃), δ (TMS, ppm): 8.07 (s, 1H), 8.03 (s, 1H), 8.00-7.93 (t, 2H), 7.89 (d, 2H), 7.76 (t, 2H), 7.61-7.52 (q, 3H), 7.39-7.33 (q, 2H), 7.24-7.03 (m, 6H), 6.91 (s, 1H), 4.56 (s, 2H), 4.49-4.36 (m, 6H), 3.71-3.57 (m, 2H), 3.35 (t, 1H).

Synthesis of (S)-4-(3-((2-((6-azidohexyl)oxy)-5-bromophenyl)diazenyl)phenyl)-1-(6-((2'-(prop-2-yn-1-yloxy)-[1,1'-binaphthalen]-2-yl)oxy)hexyl)-1H-1,2,3-triazole (8b)

8b was synthesized in a similar manner to that for 8a with the exception that 6b was used in 87.8% yield, red viscous liquid. ¹H NMR (300 MHz, CDCl₃), δ (TMS, ppm): 8.33 (s, 1H), 8.01 (d, 1H), 7.96-7.91 (t, 2H), 7.87-7.81 (q, 3H), 7.64 (s, 1H), 7.61-7.55 (m, 2H), 7.51 (m, 1H), 7.46 (s, 1H), 7.42 (d, 1H), 7.34-7.27 (m, 2H), 7.23 (t, 2H), 7.17 (t, 2H), 4.99 (d, 1H), 4.55 (m, 2H), 4.19 (t, 1H), 4.13-4.00 (m, 3H), 3.94 (q, 1H), 3.81 (t, 1H), 3.38 (m, 1H), 1.94-0.86 (m, 16H).

Synthesis of (S)-4-(3-((2-((11-azidoundecyl)oxy)-5-bromophenyl)diazenyl)phenyl)-1-(11-((2'-(prop-2-yn-1-yloxy)-[1,1'-binaphthalen]-2-yl)oxy)undecyl)-1H-1,2,3-triazole (8c)

8b was synthesized in a similar manner to that for 8a with the exception that 6b was used in 85.3% yield, red viscous liquid. ¹H NMR (300 MHz, CDCl₃), δ (TMS, ppm): 8.30 (s, 1H), 8.08 (d, 1H), 7.95 (d, 2H), 7.86 (m, 5H), 7.59-7.49 (m, 3H), 7.42 (d, 1H), 7.33 (t, 2H), 7.23-7.10 (m, 4H), 7.00 (d, 1H), 4.57 (q, 2H), 4.44 (t, 2H), 4.19-4.09 (m, 2H), 4.01-3.84 (m, 2H), 3.25 (t, 2H), 2.00-0.89 (m, 36H).

Synthesis of cyclic azobenzenophane with 2C linkers (9a)

A 1000 mL three-necked round-bottom flask was charged with 700 mL DMF followed by bubbling with Ar for 8h to remove oxygen. Then CuBr (0.42 g, 3.00 mmol) and PMDETA (0.52 g, 3.00 mmol) were charged into the flask under the protection of argon with stirring at 70 °C. The solution of 8a (2.30 g, 3.00 mmol) in DMF (15 mL) was added slowly into the CuBr/PMDETA mixture via a syringe pump under vigorous dynamoelectric stirring with the protection of Ar and then the reaction was allowed to proceed for another 10 h. The mixture was cooled to room temperature and DMF was evaporated under reduced pressure. The obtained product

was purified by column chromatography on silica gel (Chloroform/THF = 8/1) to obtain cyclic azobenzenophane 9a as yellow solid in 75.6 %. ¹H NMR (300 MHz, CDCl₃), δ (TMS, ppm): 8.13-6.77 (m, 21H), 4.86-4.21 (m, 10H). HR-MS m/z: [M]⁺ calcd for C₄₁H₃₁BrN₈O₃Na⁺, 785.1600; found, 785.1609. EA: calculated for C₄₁H₃₁BrN₈O₃: C, 64.49 %; H, 4.09 %; N, 14.67 %. Found: C, 64.95 %; H, 3.89 %; N, 14.42 %.

Synthesis of cyclic azobenzenophane with 6C linkers (9b)

9b was synthesized in a similar manner to that for 9a with the exception that 8b was used in 77.9 % yield, yellow solid. ¹H NMR (300 MHz, CDCl₃), δ (TMS, ppm): 8.29-6.90 (m, 21H), 5.13 (d, 2H), 4.16-3.85 (m, 8H), 1.84-0.96 (m, 16H). HR-MS m/z: [M]⁺ calcd for C₄₉H₄₇BrN₈O₃H⁺, 875.3233; found, 875.3020. EA: calculated for C₄₉H₄₇BrN₈O₃: C, 67.19 %; H, 5.41 %; N, 12.79 %. Found: C, 66.66 %; H, 5.52 %; N, 12.53 %.

Synthesis of cyclic azobenzenophane with 11C linkers (9c)

9c was synthesized in a similar manner to that for 9a with the exception that 8c was used in 67.5 % yield, yellow solid. ¹H NMR (300 MHz, CDCl₃), δ (TMS, ppm): 8.24-6.68 (m, 21H), 5.27 (q, 2H), 4.44 (t, 2H), 4.20-3.80 (m, 6H), 1.97-0.94 (m, 36H). HR-MS m/z: [M]⁺ calcd for C₅₉H₆₇BrN₈O₃Na⁺, 1037.4417; found, 1037.4405. EA: calculated for C₄₉H₄₇BrN₈O₃: C, 69.74 %; H, 6.65 %; N, 11.03 %. Found: C, 70.16 %; H, 6.84 %; N, 10.61 %.

Synthesis of monomer with 6C linkers (CM)

A 50 mL Schlenk tube was charged with 1.49 g (1.70 mmol) 9b, 0.75 g (5.10 mmol) 4-vinylphenylboronic acid, and 40 mg (2 % eq.) tetrakis(triphenylphosphine) palladium(0) and 20 mL THF, then after the addition of 12.5 mL 1M sodium carbonate solution, the mixture was freeze-pump-thaw three times and stirred at 90 °C for 24 h. After cooling to room temperature the mixture was poured into 100 mL

CH₂Cl₂, washed with water three times and the solvent of the organic layers were removed under reduced pressure. The obtained product was purified by column chromatography on silica gel (Chloroform/THF = 10/1) to obtain monomer CM as yellow solid in 83.0 % yield. ¹H NMR (300 MHz, CDCl₃), δ (TMS, ppm): 8.30-6.73 (m, 26H), 5.82 (d, 1H), 5.29 (d, 1H), 5.15 (q, 2H), 4.23-3.84 (m, 8H), 1.87-0.96 (m, 16H). ¹³C NMR (75 MHz, CDCl₃), δ (TMS, ppm): 156.13, 154.31, 153.90, 153.65, 146.95, 144.66, 142.78, 139.49, 136.46, 136.41, 134.16, 134.09, 133.50, 131.75, 130.77, 129.67, 129.63, 129.53, 129.30, 129.26, 128.00, 127.91, 127.44, 126.89, 126.72, 126.67, 126.44, 126.34, 125.56, 125.32, 123.99, 123.67, 122.37, 121.25, 120.28, 120.16, 116.59, 115.57, 115.37, 115.07, 114.93, 113.88, 69.62, 68.78, 64.27, 49.98, 49.85, 49.75, 29.89, 29.73, 29.54, 29.08, 28.57, 26.14, 25.69, 24.94, 24.27. HR-MS m/z: [M]⁺ calcd for C₅₇H₅₄N₈O₃H⁺, 899.4397; found, 899.4375. EA: calculated for C₅₇H₅₄N₈O₃: C, 76.14 %; H, 6.05 %; N, 12.46 %. Found: C, 76.49 %; H, 6.23 %; N, 12.25 %. Melting point (*T*_m): 128.5-130.0 °C.

Synthesis of monomer with 2C linkers (CM1)

A 50 mL Schlenk tube was charged with 1.30 g (1.70 mmol) 9a, 0.75 g (5.10 mmol) 4-vinylphenylboronic acid, and 40 mg (2 % eq.) tetrakis(triphenylphosphine) palladium(0) and 20 mL THF, then after the addition of 12.5 mL 1M sodium carbonate solution, the mixture was freeze-pump-thaw three times and stirred at 90 °C for 24 h. After cooling to room temperature the mixture was poured into 100 mL CH₂Cl₂, washed with water three times and the solvent of the organic layers were removed under reduced pressure. The obtained product was purified by column chromatography on silica gel (Chloroform/THF = 5/1) to obtain monomer CM1 as yellow solid in 76.5 % yield. ¹H NMR (300 MHz, CDCl₃), δ(TMS, ppm): 8.15-6.83 (m, 25H), 6.78 (q, 1H), 5.83 (d, 1H), 5.31 (d, 1H), 4.85-4.29 (m, 10H). ¹³C NMR (75 MHz, CDCl₃), δ(TMS, ppm): 155.06, 153.99, 153.34, 152.77, 146.41, 143.72, 142.13, 139.19, 136.63, 136.32, 134.35, 133.80, 133.76, 132.06, 130.89, 129.79, 129.53, 129.45, 129.23, 128.86, 127.87, 127.82, 126.93, 126.72, 126.26, 125.20, 125.08,

125.00, 124.08, 123.99, 122.38, 120.96, 119.70, 117.98, 115.19, 114.11, 114.00, 113.72, 67.41, 66.89, 63.76, 49.83, 49.64 (Some peaks overlapped). HR-MS m/z : $[M]^+$ calcd for $C_{57}H_{54}N_8O_3H^+$, 787.3145; found, 787.3130. EA: calculated for $C_{57}H_{54}N_8O_3$: C, 74.79 %; H, 4.87 %; N, 14.24 %. Found: C, 74.63 %; H, 5.09 %; N, 14.45 %. Melting point (T_m): 167.0-169.0 °C.

Synthesis of monomer with 11C linkers (CM2)

A 50 mL Schlenk tube was charged with 1.77 g (1.70 mmol) 9a, 0.75 g (5.10 mmol) 4-vinylphenylboronic acid, and 40 mg (2 % eq.) tetrakis(triphenylphosphine) palladium(0) and 20 mL THF, then after the addition of 12.5 mL 1M sodium carbonate solution, the mixture was freeze-pump-thaw three times and stirred at 90 °C for 24 h. After cooling to room temperature the mixture was poured into 100 mL CH_2Cl_2 , washed with water three times and the solvent of the organic layers were removed under reduced pressure. The obtained product was purified by column chromatography on silica gel (Chloroform/THF = 20/1) to obtain monomer CM2k as yellow solid in 86.8 % yield. 1H NMR (300 MHz, $CDCl_3$), δ (TMS, ppm): 8.26-6.70 (m, 26H), 5.82 (d, 1H), 5.29 (d, 1H), 5.22 (q, 2H), 4.44-3.39 (t, 2H), 4.26-3.80 (m, 6H), 1.95-0.94 (m, 36H). ^{13}C NMR (75 MHz, $CDCl_3$), δ (TMS, ppm): 156.30, 154.53, 153.58, 153.47, 147.22, 145.18, 142.61, 139.50, 136.42, 134.18, 134.12, 133.37, 131.77, 130.75, 129.64, 129.57, 129.28, 128.02, 127.92, 126.86, 126.71, 126.39, 126.30, 125.47, 125.45, 125.28, 123.83, 123.68, 122.07, 120.88, 120.52, 119.99, 117.54, 115.97, 115.81, 115.22, 114.99, 113.84, 69.88, 69.79, 64.14, 50.47, 50.14, 30.24, 30.11, 29.54, 29.44, 29.41, 29.37, 29.31, 29.16, 29.11, 29.05, 29.03, 28.86, 26.37, 26.14, 25.44 (Some peaks overlapped). LC-MS m/z : $[M]^+$ calcd for $C_{57}H_{54}N_8O_3H^+$, 1039.5962; found, 1039.5987. EA: calculated for $C_{57}H_{54}N_8O_3$: C, 77.42 %; H, 7.18 %; N, 10.78 %. Found: C, 77.03 %; H, 7.29 %; N, 11.07 %. Melting point (T_m): 122.0-123.0 °C.

Synthesis of polymers PCM, PCM1 and PCM2

The polymers were prepared via the similar procedure: According to a predetermined molar ratio ($[\text{Monomer}]_0: [\text{AIBN}]_0 = 30:1$), monomer, AIBN and THF was added into a dry ampule tube. The contents were freeze-pump-thaw three times to eliminate the oxygen. Then the ampule was flame-sealed and stirred in an oil bath by a thermostat at 80 °C for 24 h. After this, the ampule was cooled at room temperature and opened afterwards. The contents were precipitated into 100 mL ethyl acetate and the precipitates were filtrated and dried to a constant weight at room temperature in vacuum.

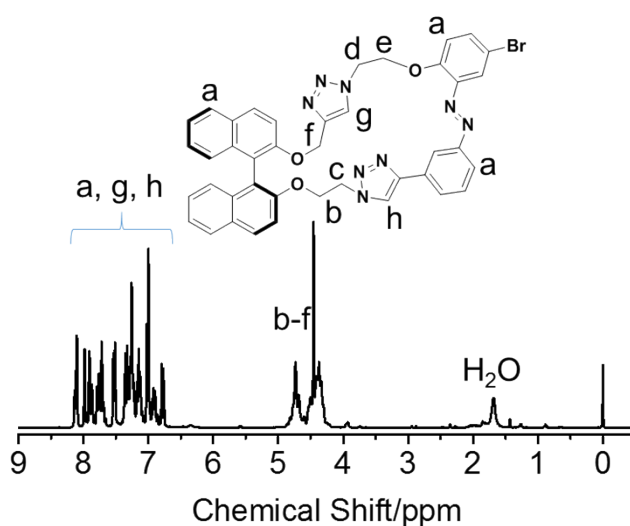


Figure S1. ^1H NMR spectrum of 9a in CDCl_3 .

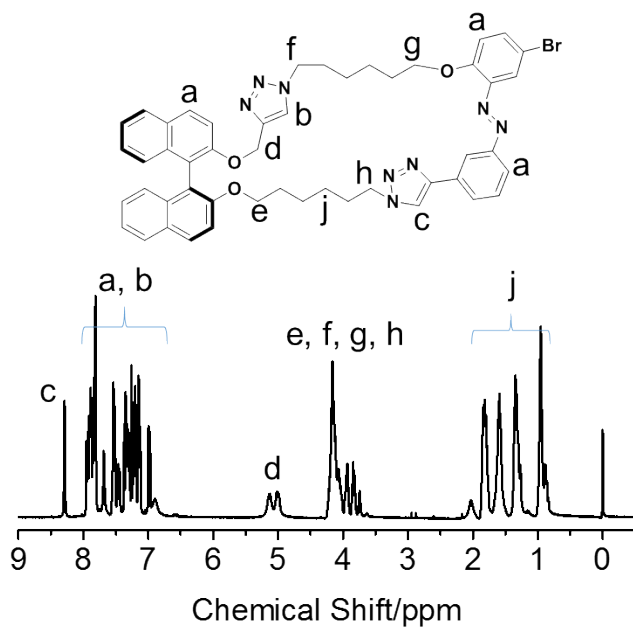


Figure S2. ¹H NMR spectrum of 9b in CDCl₃.

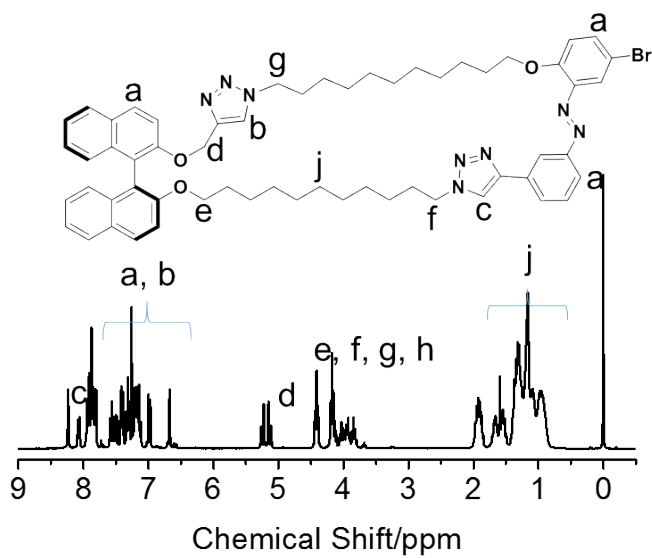


Figure S3. ¹H NMR spectrum of 9c in CDCl₃.

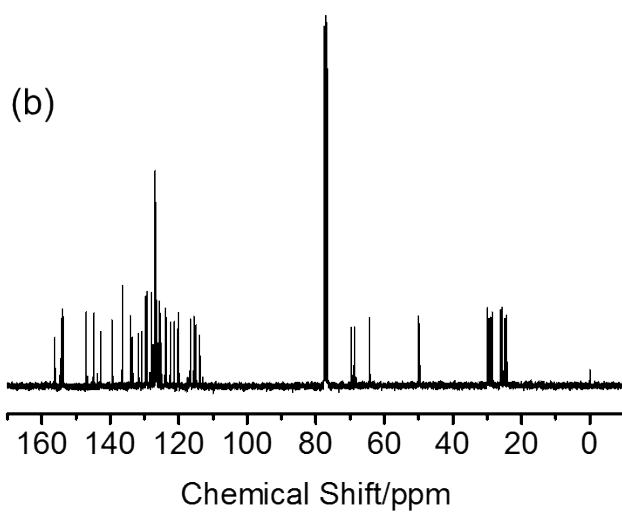
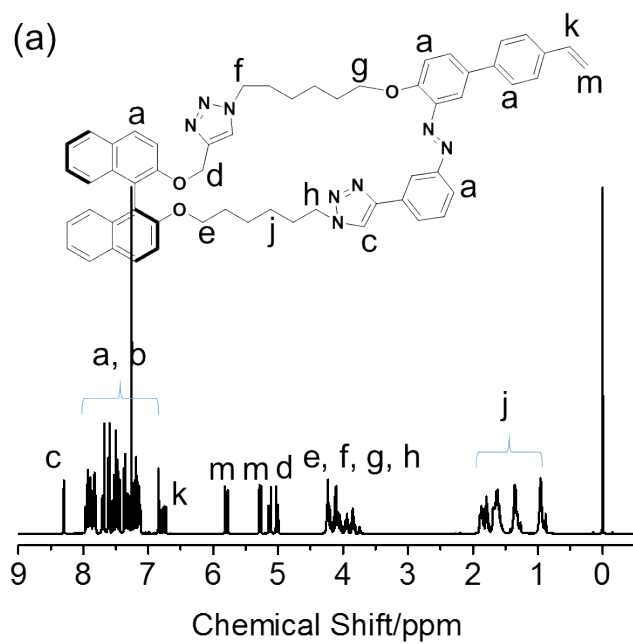


Figure S4. ^1H NMR spectrum (a) and ^{13}C NMR spectrum (b) of CM in CDCl_3 .

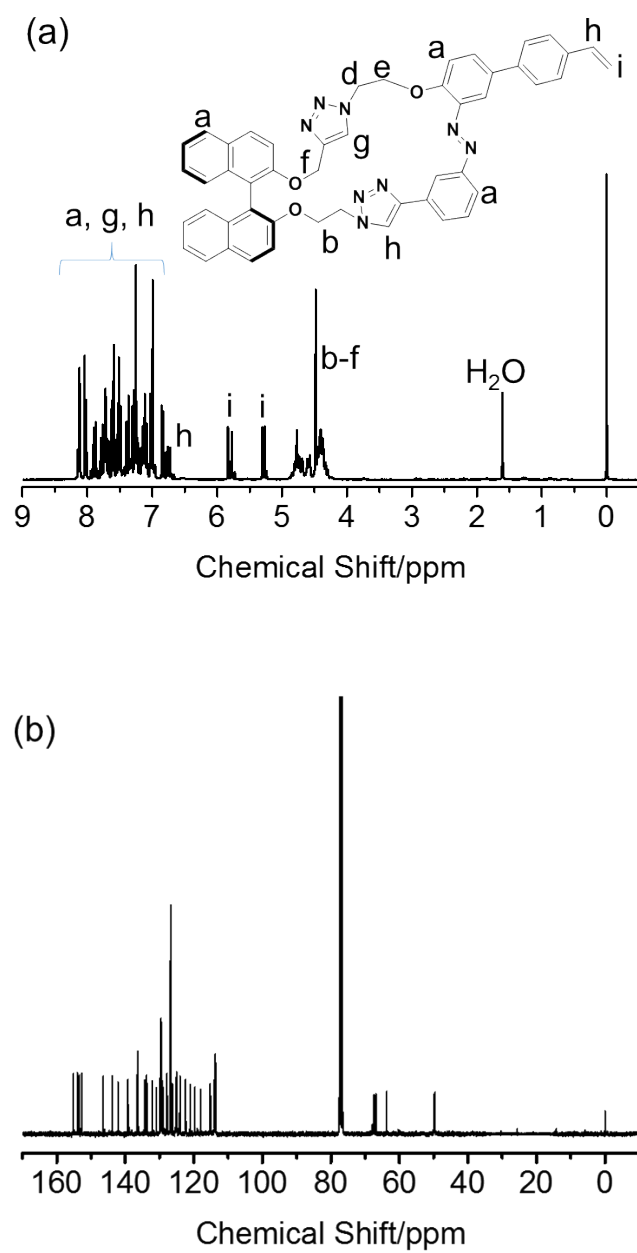


Figure S5. ^1H NMR spectrum (a) and ^{13}C NMR spectrum (b) of CM1 in CDCl_3 .

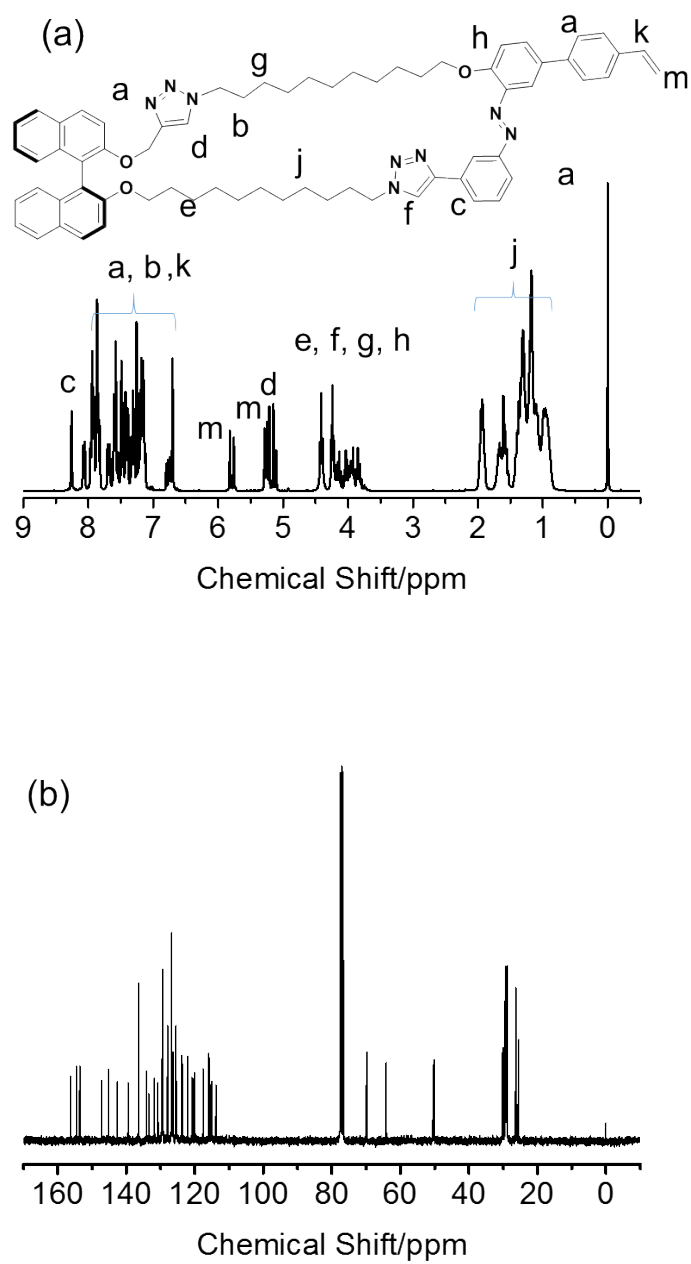


Figure S6. ¹H NMR spectrum (a) and ¹³C NMR spectrum (b) of CM2 in CDCl₃.

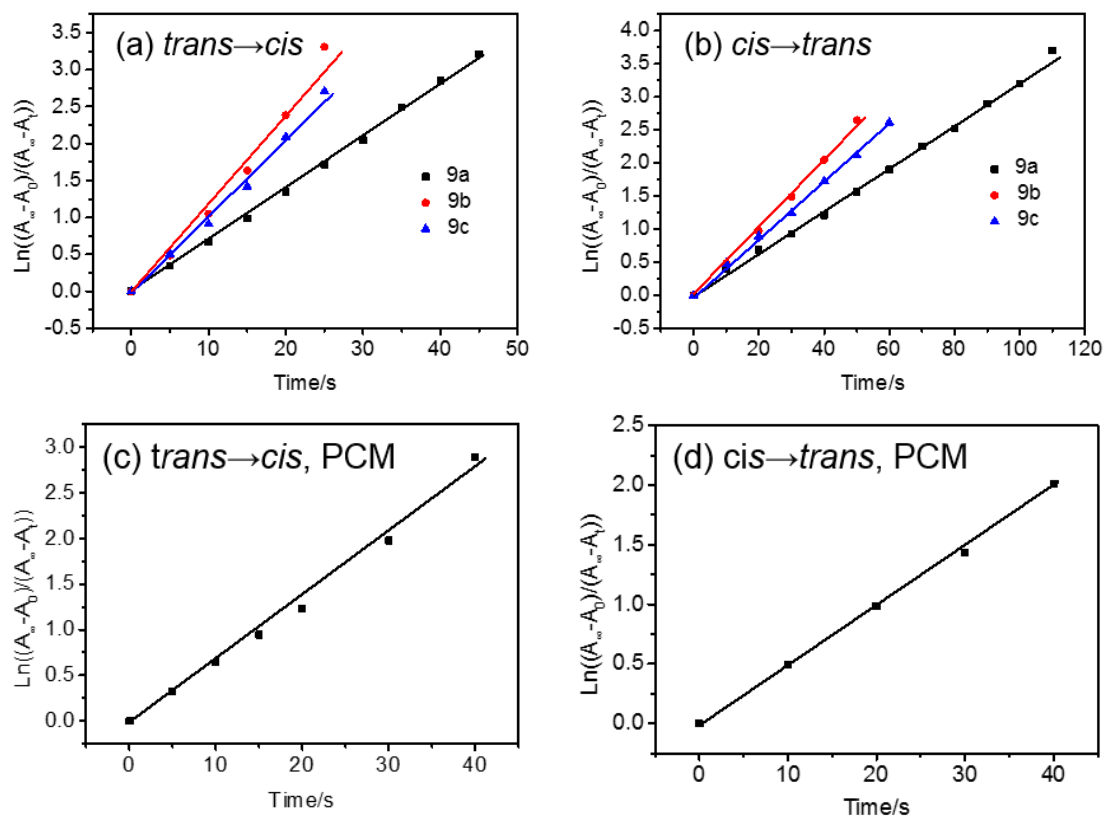


Figure S7. The first-order kinetics of *trans*-to-*cis* and *cis*-to-*trans* photoisomerization processes of azobenzene segments. (a) and (c): *trans*-to-*cis* isomerization of 9a-c and PCM in chloroform during the irradiation with the 365 nm light (light intensity: 10 mW/cm²); (b) and (d): *cis*-to-*trans* isomerization of 9a-c and PCM in chloroform during the irradiation with the 435 nm light (light intensity: 3.6 mW/cm²) at room temperature.

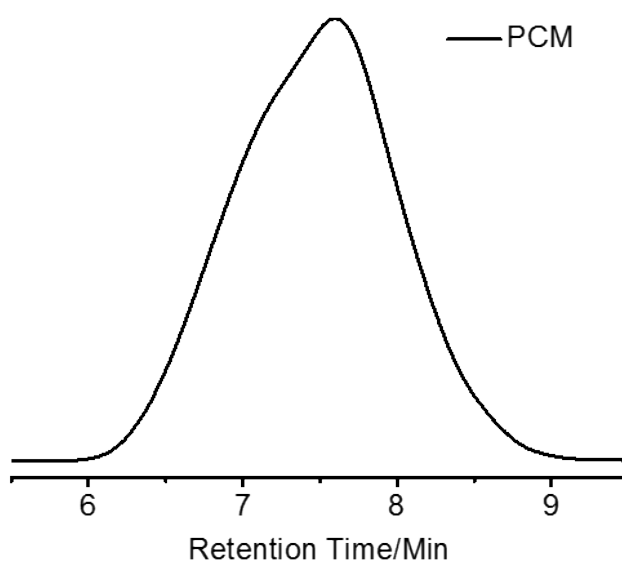


Figure S8. GPC trace of PCM ($M_n = 15000$ g/mol, $M_w/M_n = 1.44$).

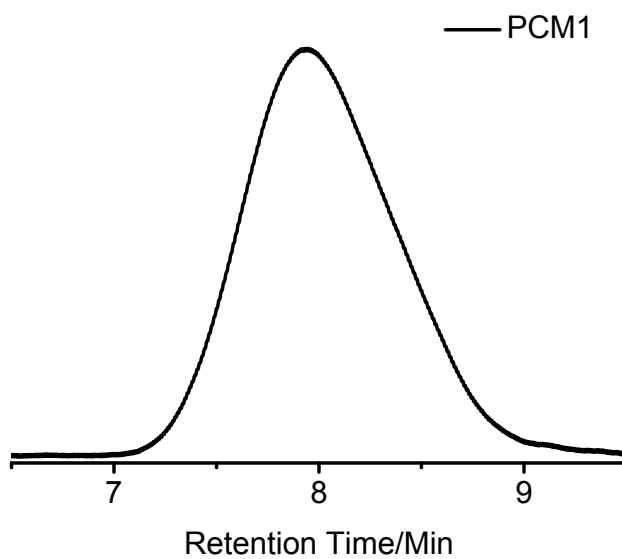


Figure S9 GPC elution curve of PCM1 with DMF as eluent ($M_n = 16000$ g/mol, $M_w/M_n = 1.43$).

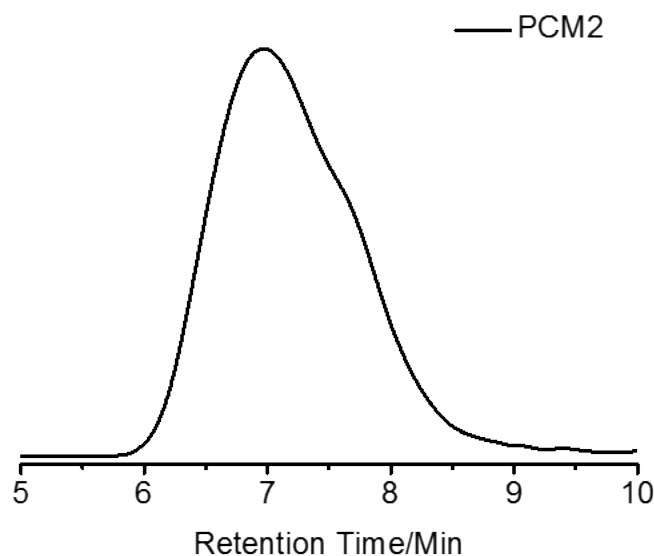


Figure S10. GPC elution curve of PCM2 with THF as eluent ($M_n = 10400$ g/mol, $M_w/M_n = 1.32$).

Table S1. $[\alpha]_D$ of PCM1 and PCM2 before and after photoirradiation^a

| Comp. | Solvent | Initial state | After 365 nm irradiation | After 436 nm irradiation | $\Delta[\alpha]_D / [\alpha]_D^b$ (%) |
|-------|-------------------|---------------|--------------------------|--------------------------|---------------------------------------|
| PCM1 | DMF | -70 | -61 | -73 | 12.8 |
| PCM2 | CHCl ₃ | -60 | -56 | -58 | 6.7 |

^a Conditions: $c = 0.10$ g/dL, 20 °C, in CHCl₃ or DMF, light path length = 10 cm, irradiation wavelength = 365 nm (10 mW/cm², 600 s) and 436 nm (3.6 mW/cm², 600 s). ^b Percent change in $[\alpha]_D$ observed in going from the initial state to PSS_{uv}.

Computational Studies

All calculations on cyclic azobenzenophanes 9a-c were carried out by using density functional theory (DFT) and time-dependent DFT (TDDFT).^[2] Figures S11-S16 show the plots of the most representative molecular frontier orbitals for 9a-c. Other relevant frontier orbitals are available in Supporting Information. Tables S2-S7 summarizes the spin-allowed electronic transitions calculated with the TDDFT method. For all the compounds, the calculated transitions agree with the experimental ones.

The HOMO and LUMO of molecules 9a-c all predominately delocalize on the

binaphthyl (bin), azobenzene (azo), triazole (N3), and phenyl (ph) moieties. As listed in Table S2-S7, the UV-vis absorption band at about 500 nm are of $\pi_{\text{azo}} \rightarrow \pi_{\text{azo}}^*$ character, probably with some mixing of a charge transfer character from the bin ring to the azo group and from the N3 ring to the azo group.

According to DFT and TDDFT calculations, the lowest energy band experimentally found for complex *9a-trans* around 489 nm mainly originate from HOMO-8 \rightarrow LUMO transitions, which can be assigned to $\pi_{\text{azo}}^* \rightarrow \pi_{\text{azo}}^*$ due to their orbital characters of the corresponding starting and arriving states (See Figures S11 and Table S2). In the UV-vis spectra, the absorption at 300 nm may come from the HOMO-3 \rightarrow LUMO transition ($\pi \rightarrow \pi^*$). The characteristic azobenzene of HOMO-3 and azobenzene groups characteristic of LUMO indicate that the HOMO-3 \rightarrow LUMO absorption transition possesses a intramolecular charge transfer (ICT) character; while the HOMO \rightarrow LUMO+1 transition is mainly on binaphthyl group, which suggests such transitions are of a $\pi_{\text{bin}} \rightarrow \pi_{\text{bin}}^*$ character at 282 nm. The experimental absorption band for complex *9a-trans* at 250 nm is also of ICT character, relevant to the calculated bands at 235 and 228 nm dominantly on phenyl of azobenzene group also suggests a $\pi_{\text{azo}} \rightarrow \pi_{\text{ph}}^*$ character, coming from a mixed transition of HOMO-2 \rightarrow LUMO+3.

According to the calculations, the experimentally observed absorption band (around 458 nm) for complex *9a-cis* mainly originates from a mixed transition of HOMO-2 \rightarrow LUMO and HOMO-3 \rightarrow LUMO. Such transition can be also assigned to intramolecular charge transfer (ICT) and $\pi \rightarrow \pi^*$ character, due to their orbital characters of the corresponding starting and arriving states. Similarly, the other observed absorptions possess a intramolecular charge transfer (ICT) character. As for the *trans* \rightarrow *cis* states of *9a*, the calculations reveal that the absorptions all follow the experimental trends (Figures S11-S12). Similar results are also found for *9b-c*, which agreed well with the experimental results.

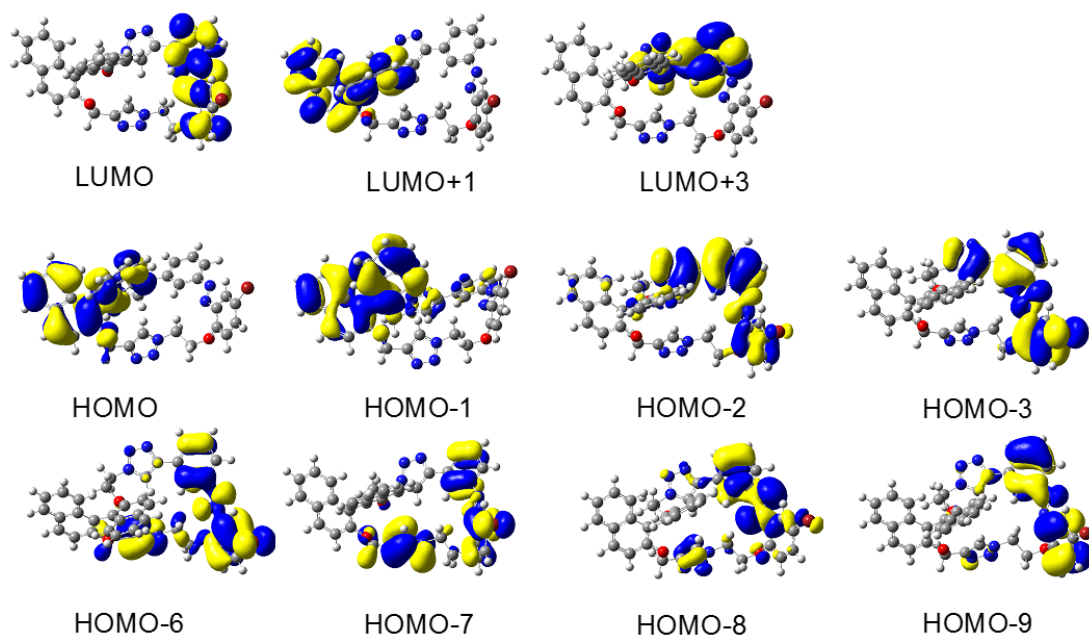


Figure S11. The graphical representation for molecular orbitals of complex 9a-*trans*.

Table S2. Main Calculated Optical Transitions for 9a-*trans*.

| Orbital Excitations | Character | Calcd/nm | f^a | Exptl/nm |
|----------------------------|--|----------|--------|----------|
| HOMO-8→LUMO | $\pi_{\text{azo}} \rightarrow \pi_{\text{azo}}^*$ | 489 | 0.0125 | 369 |
| HOMO-3→LUMO | $\pi_{\text{azo}} \rightarrow \pi_{\text{azo}}^*$ $\pi_{\text{N}_3} \rightarrow \pi_{\text{azo}}^*$ | 300 | 0.3195 | |
| HOMO→LUMO+1 | $\pi_{\text{bin}} \rightarrow \pi_{\text{bin}}^*$ $\pi_{\text{N}_3} \rightarrow \pi_{\text{bin}}^*$ | 282 | 0.1845 | 284 |
| HOMO-6→LUMO HOMO-7→LUMO | $\pi_{\text{azo}} \rightarrow \pi_{\text{azo}}^*$ $\pi_{\text{N}_3} \rightarrow \pi_{\text{azo}}^*$ | 270 | 0.1762 | 266 |
| HOMO-1→LUMO+1 | $\pi_{\text{bin}} \rightarrow \pi_{\text{bin}}^*$ | 253 | 0.0123 | |
| HOMO-9→LUMO | $\pi_{\text{bin}} \rightarrow \pi_{\text{azo}}^*$ | 235 | 0.0834 | 242 |
| HOMO-2→LUMO+3 | $\pi_{\text{azo}} \rightarrow \pi_{\text{ph}}^*$ $\pi_{\text{N}_3} \rightarrow \pi_{\text{N}_3}^*$ | 228 | 0.4092 | |

^a Oscillator strength.

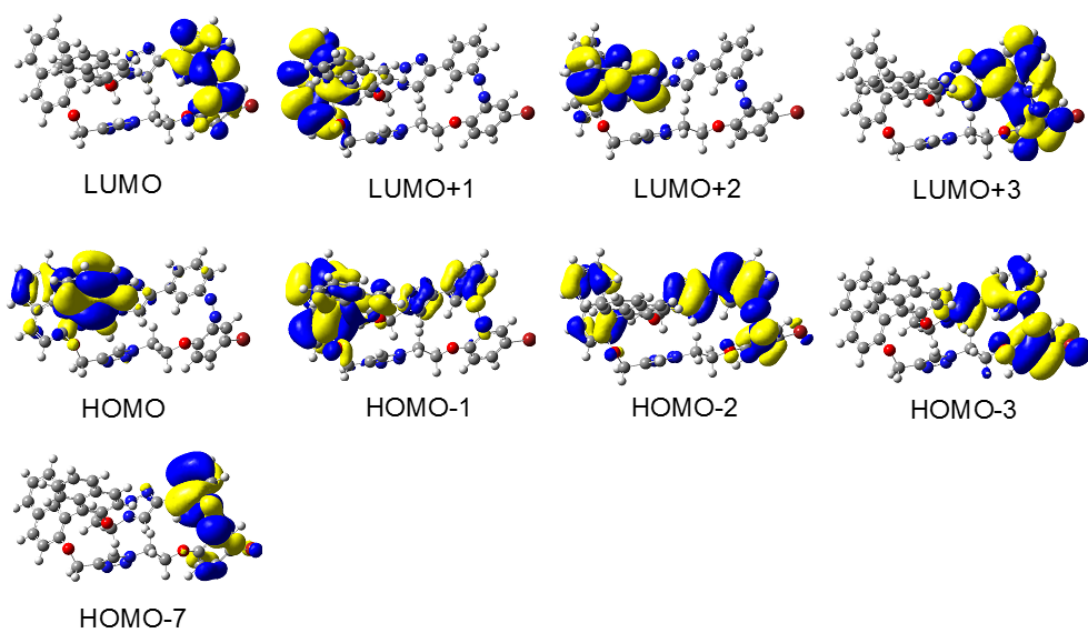


Figure S12. The graphical representation for molecular orbitals of complex 9a-cis.

Table S3. Main Calculated Optical Transitions for 9a-cis.

| Orbital Excitations | Character | Calcd/nm | f^a | Exptl/nm |
|------------------------------|---|----------|--------|----------|
| HOMO-2→LUMO HOMO-3→LUMO | $\pi_{\text{bin}} \rightarrow \pi_{\text{azo}}^*$ $\pi_{\text{azo}} \rightarrow \pi_{\text{azo}}^*$ $\pi_{\text{N}_3} \rightarrow \pi_{\text{azo}}^*$ | 458 | 0.0061 | 352 |
| HOMO→LUMO+2 | $\pi_{\text{bin}} \rightarrow \pi_{\text{bin}}^*$ | 274 | 0.1022 | 270 |
| HOMO-1→LUMO+1 HOMO→LUMO+1 | $\pi_{\text{bin}} \rightarrow \pi_{\text{bin}}^*$ $\pi_{\text{azo}} \rightarrow \pi_{\text{bin}}^*$ $\pi_{\text{N}_3} \rightarrow \pi_{\text{bin}}^*$ | 259 | 0.0854 | |
| HOMO-7→LUMO | $\pi_{\text{azo}} \rightarrow \pi_{\text{azo}}^*$ | 252 | 0.0998 | 242 |
| HOMO-3→LUMO+3 | $\pi_{\text{azo}} \rightarrow \pi_{\text{azo}}^*$ $\pi_{\text{N}_3} \rightarrow \pi_{\text{azo}}^*$ | 244 | 0.0394 | |
| HOMO-2→LUMO+3 | $\pi_{\text{azo}} \rightarrow \pi_{\text{azo}}^*$ $\pi_{\text{bin}} \rightarrow \pi_{\text{azo}}^*$ $\pi_{\text{N}_3} \rightarrow \pi_{\text{azo}}^*$ | 237 | 0.3959 | |

^a Oscillator strength.

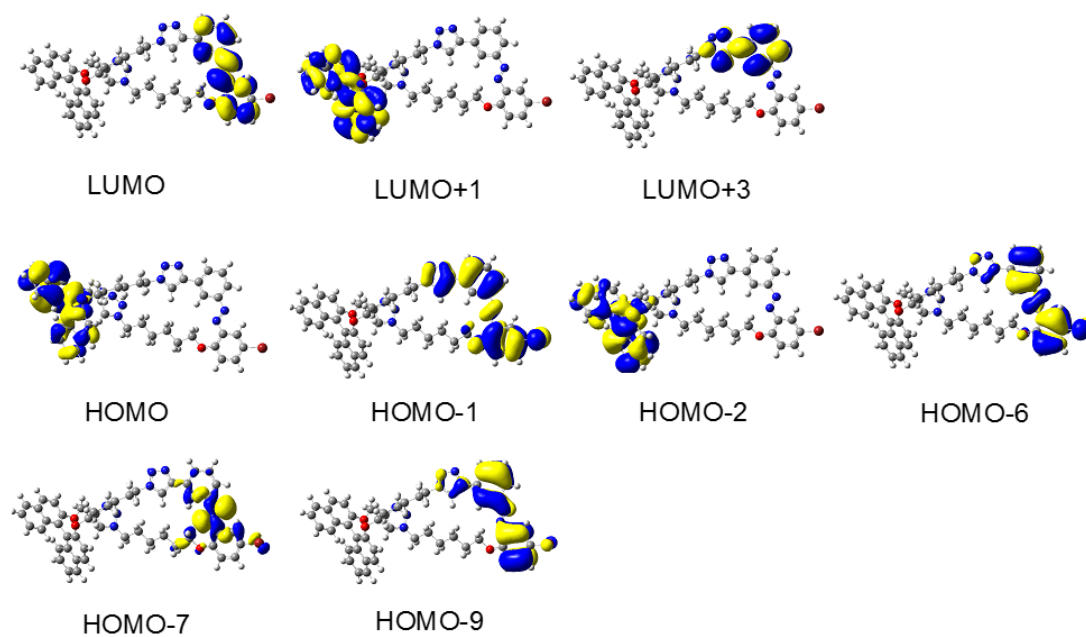


Figure S13. The graphical representation for molecular orbitals of complex 9b-*trans*.

Table S4. Main Calculated Optical Transitions for 9b-*trans*.

| Orbital Excitations | Character | Calcd/nm | f^a | Exptl/nm |
|---------------------|--|----------|--------|----------|
| HOMO-7→LUMO | $\pi_{\text{azo}} \rightarrow \pi_{\text{azo}}^*$ | 487 | 0.0001 | 372 |
| HOMO-1→LUMO | $\pi_{\text{azo}} \rightarrow \pi_{\text{azo}}^*$ $\pi_{\text{N}_3} \rightarrow \pi_{\text{azo}}^*$ | 325 | 0.5062 | |
| HOMO→LUMO+1 | $\pi_{\text{bin}} \rightarrow \pi_{\text{bin}}^*$ | 286 | 0.1627 | 283 |
| HOMO-6→LUMO | $\pi_{\text{azo}} \rightarrow \pi_{\text{azo}}^*$ | 276 | 0.2629 | 270 |
| HOMO-2→LUMO+1 | $\pi_{\text{bin}} \rightarrow \pi_{\text{bin}}^*$ | 253 | 0.0324 | |
| HOMO-2→LUMO | $\pi_{\text{bin}} \rightarrow \pi_{\text{azo}}^*$ | 232 | 0.2323 | 243 |
| HOMO-1→LUMO+3 | $\pi_{\text{azo}} \rightarrow \pi_{\text{N}_3}^*$ $\pi_{\text{N}_3} \rightarrow \pi_{\text{N}_3}^*$ | | | |
| HOMO-9→LUMO | $\pi_{\text{azo}} \rightarrow \pi_{\text{azo}}^*$ | | | |

^a Oscillator strength.

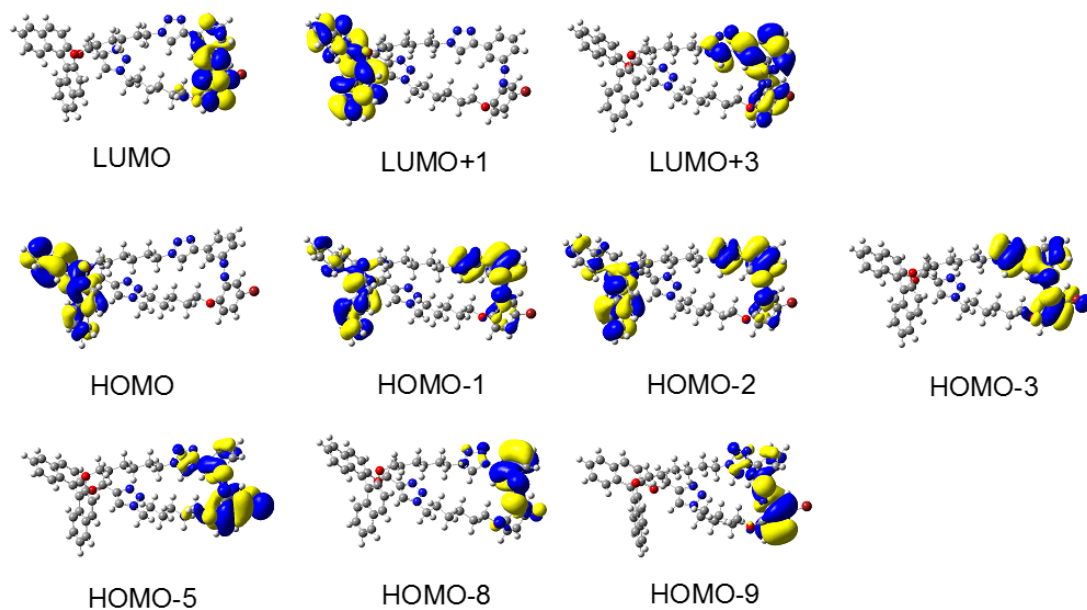


Figure S14. The graphical representation for molecular orbitals of complex 9b-*cis*.

Table S5. Main Calculated Optical Transitions for 9b-*cis*.

| Orbital Excitations | Character | Calcd/nm | f^a | Exptl/nm |
|---------------------|---|----------|--------|----------|
| HOMO-1→LUMO | $\pi_{\text{bin}} \rightarrow \pi_{\text{azo}}^*$ | 502 | 0.0135 | 441 |
| HOMO-2→LUMO | $\pi_{\text{azo}} \rightarrow \pi_{\text{azo}}^*$ | | | |
| HOMO→LUMO+1 | $\pi_{\text{bin}} \rightarrow \pi_{\text{bin}}^*$ | 286 | 0.1632 | 282 |
| HOMO-5→LUMO | $\pi_{\text{azo}} \rightarrow \pi_{\text{azo}}^*$ | 272 | 0.0571 | |
| HOMO-8→LUMO | $\pi_{\text{azo}} \rightarrow \pi_{\text{azo}}^*$ | 263 | 0.0999 | 242 |
| HOMO-9→LUMO+3 | $\pi_{\text{azo}} \rightarrow \pi_{\text{azo}}^*$ | 245 | 0.1571 | |
| | $\pi_{\text{N}_3} \rightarrow \pi_{\text{azo}}^*$ | | | |
| HOMO-2→LUMO+3 | $\pi_{\text{bin}} \rightarrow \pi_{\text{azo}}^*$ | 241 | 0.2406 | |
| HOMO-1→LUMO+3 | $\pi_{\text{azo}} \rightarrow \pi_{\text{azo}}^*$ | | | |
| HOMO-3→LUMO+3 | $\pi_{\text{azo}} \rightarrow \pi_{\text{azo}}^*$ | 225 | 0.2388 | NA |
| | $\pi_{\text{N}_3} \rightarrow \pi_{\text{azo}}^*$ | | | |

^a Oscillator strength.

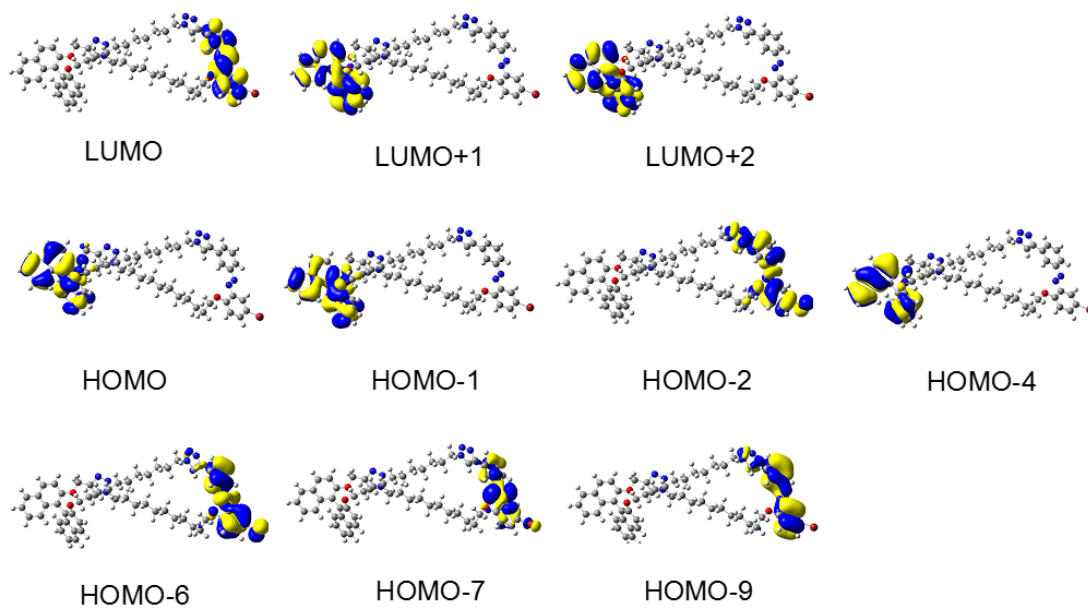


Figure S15. The graphical representation for molecular orbitals of complex *9c-trans*.

Table S6. Main Calculated Optical Transitions for *9c-trans*.

| Orbital Excitations | Character | Calcd/nm | f^a | Exptl/nm |
|---------------------|--|----------|--------|----------|
| HOMO-7→LUMO | $\pi_{\text{azo}} \rightarrow \pi_{\text{azo}}^*$ | 502 | 0.0015 | 372 |
| HOMO-2→LUMO | $\pi_{\text{azo}} \rightarrow \pi_{\text{azo}}^*$ $\pi_{\text{N}_3} \rightarrow \pi_{\text{azo}}^*$ | 324 | 0.5330 | |
| HOMO→LUMO+1 | $\pi_{\text{bin}} \rightarrow \pi_{\text{bin}}^*$ | 287 | 0.1887 | 282 |
| HOMO-6→LUMO | $\pi_{\text{azo}} \rightarrow \pi_{\text{azo}}^*$ | 275 | 0.2701 | 242 |
| HOMO-1→LUMO+2 | $\pi_{\text{bin}} \rightarrow \pi_{\text{bin}}^*$ | 251 | 0.0392 | NA |
| HOMO-9→LUMO | $\pi_{\text{azo}} \rightarrow \pi_{\text{azo}}^*$ | 224 | 0.3739 | |
| HOMO-4→LUMO+1 | $\pi_{\text{bin}} \rightarrow \pi_{\text{bin}}^*$ | 214 | 0.6306 | |

^a Oscillator strength.

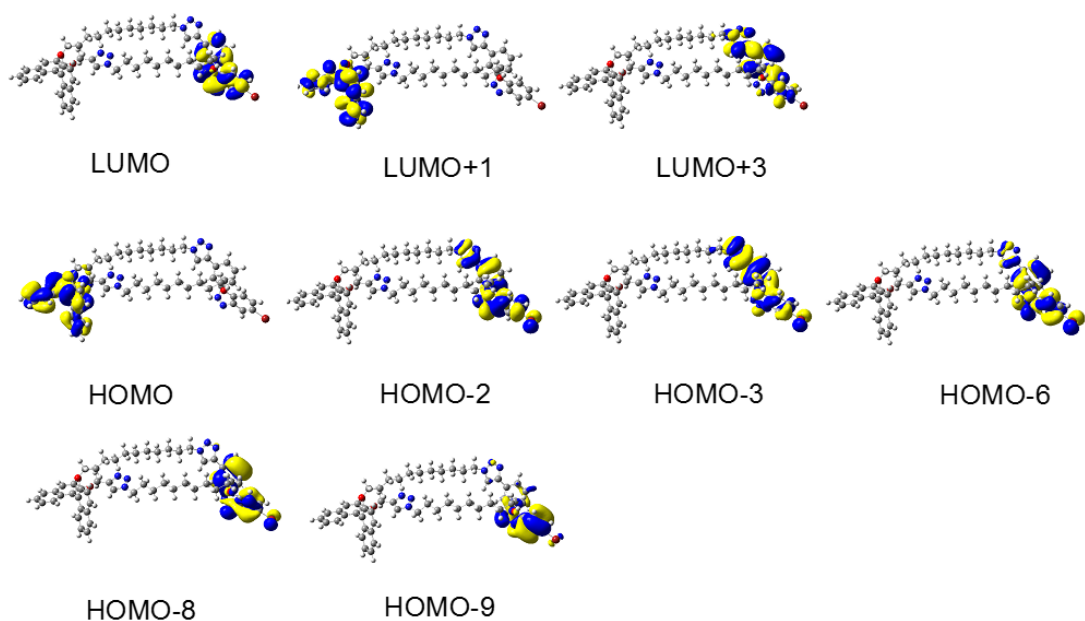


Figure S16. The graphical representation for molecular orbitals of complex *9c-cis*.

Table S7. Main Calculated Optical Transitions for *9c-cis*.

| Orbital Excitations | Character | Calcd/nm | f^a | Exptl/nm |
|---------------------|---|----------|--------|----------|
| HOMO-2→LUMO | $\pi_{\text{azo}} \rightarrow \pi_{\text{azo}}^*$ $\pi_{\text{N3}} \rightarrow \pi_{\text{azo}}^*$ | 485 | 0.0112 | 372 |
| HOMO→LUMO+1 | $\pi_{\text{bin}} \rightarrow \pi_{\text{bin}}^*$ | 285 | 0.1794 | 280 |
| HOMO-3→LUMO | $\pi_{\text{azo}} \rightarrow \pi_{\text{azo}}^*$ | 268 | 0.0431 | |
| HOMO-8→LUMO | $\pi_{\text{azo}} \rightarrow \pi_{\text{azo}}^*$ | 256 | 0.0477 | 242 |
| HOMO-2→LUMO+3 | $\pi_{\text{azo}} \rightarrow \pi_{\text{azo}}^*$ $\pi_{\text{N3}} \rightarrow \pi_{\text{azo}}^*$ | 247 | 0.0602 | |
| HOMO-8→LUMO | $\pi_{\text{azo}} \rightarrow \pi_{\text{azo}}^*$ | 234 | 0.6477 | |
| HOMO-2→LUMO+3 | $\pi_{\text{N3}} \rightarrow \pi_{\text{azo}}^*$ | | | |
| HOMO-6→LUMO+3 | $\pi_{\text{azo}} \rightarrow \pi_{\text{azo}}^*$ | 223 | 0.1254 | NA |

^a Oscillator strength.

- (1) Li, J.; Zhou, N.; Zhang, Z.; Xu, Y.; Chen, X.; Tu, Y.; Hu, Z.; Zhu, X. *Chem.-Asian J.* **2013**, *8*, 1095-1100.
- (2) Frisch, M. J.; Trucks, G. W.; Schlegel, H. B.; Scuseria, G. E.; Robb, M. A.; Cheeseman, J. R.; Scalmani, G.; Barone, V.; Mennucci, B.; Petersson, G. A.; Nakatsuji, H.; Caricato, M.; Li, X.; Hratchian, H. P.; Izmaylov, A. F.; Bloino, J.; Zheng, G.; Sonnenberg, J. L.; Hada, M.; Ehara, M.; Toyota, K.; Fukuda, R.; Hasegawa, J.; Ishida, M.; Nakajima, T.; Honda, Y.; Kitao, O.; Nakai, H.; Vreven, T.; Montgomery, Jr., J. A.; Peralta, J. E.; Ogliaro, F.; Bearpark, M.; Heyd, J. J.; Brothers, E.; Kudin, K. N.; Staroverov, V. N.; Keith, T.; Kobayashi, R.; Normand, J.; Raghavachari, K.; Rendell, A.; Burant, J. C.; Iyengar, S. S.; Tomasi, J.; Cossi, M.; Rega, N.; Millam, J. M.; Klene, M.; Knox, J. E.; Cross, J. B.; Bakken, V.; Adamo, C.; Jaramillo, J.; Gomperts, R.; Stratmann, R. E.; Yazyev, O.; Austin, A. J.; Cammi, R.; Pomelli, C.; Ochterski, J. W.; Martin, R. L.; Morokuma, K.; Zakrzewski, V. G.; Voth, G. A.; Salvador, P.; Dannenberg, J. J.; Dapprich, S.; Daniels, A. D.; Farkas, O.; Foresman, J. B.; Ortiz, J. V.; Cioslowski, J.; Fox, D. J. Gaussian 09, revision C.01; Gaussian, Inc.: Wallingford, CT, 2010.